4. AUTOMOTIVE METALS – TITANIUM

A. Low-Cost Titanium Powder for Feedstock

Principal Investigator(s): Curt A. Lavender and K. Scott Weil
Pacific Northwest National Laboratory (PNNL)
Richland, WA 99352
(509) 372-6770; fax: (509) 375-4448; e-mail: curt.lavender@pnl.gov
(509) 375-6796; fax: (509)375-4448; e-mail: scott.weil@pnl.gov

Technology Area Development Manager: Joseph A. Carpenter
(202) 586-1022; fax: (202) 586-1600; e-mail: joseph.carpenter@ee.doe.gov

Expert Technical Monitor: Philip S. Sklad
(865) 574-5069; fax: (865) 576-4963; e-mail: skladps@ornl.gov

Participants:
Lance Jacobsen, International Ti Powder, Inc., 20634 W. Gasken Drive, Lockport, IL 60441
Michael Hyzny, DuPont, (302) 999-5252 e-mail:michael.t.hyzny@USA.dupont.com
Tim Soran, ATI Allvac, (509) 372-1711; e-mail:Tim.Soran@Allvac.com

Contractor: PNNL
Contract No.: DE-AC06-76RLO1830

Objective

- Investigate alternate powder and melt-processing methods for low-cost titanium (Ti) materials.
- Evaluate processing methods to produce powder metallurgy (P/M) Ti products with International Ti Powder, Inc. (ITP) powders.
- Evaluate the suitability of emerging Ti technologies for the production of low-cost Ti products for automotive applications.

Approach

- Perform characterization and analysis of the sintering behavior of commercial-purity (CP)-Ti and Ti-alloy ITP powder. Provide feedback of results to ITP for use in process design.
- Develop low-cost feedstock for P/M use in automotive applications from low-cost Ti tetrachloride ($TiCl_4$).
- Survey the emerging technologies for the low-cost production of Ti powders and evaluate for use in automotive applications.

Accomplishments

- Observed decreased swelling in a series of lower-purity, $TiCl_4$-produced powders relative to those synthesized from standard $TiCl_4$. The improvement is attributed to the increase in the onset of sintering temperature, which mitigates the entrapment of volatile impurities that would otherwise lead to pore formation and growth. The net effect is that the use of a lower-purity $TiCl_4$ may be beneficial in two ways: (1) it is a potentially lower-cost precursor to Ti powder production and (2) the trace impurities allow higher-density components to be fabricated via a typical, low-cost, press-and-sinter approach. Preliminary mechanical test results indicate that the impurities have no effect on tensile strength.

- An instrumented powder-pressing die was fabricated and used in die-pressing experiments, to measure the effectiveness of in-die and admixed powder lubrication in increasing green body density and reducing pressing pressure.
- The ITP powder particle-size distribution was modified by various milling techniques, including Spex, attrition and ball milling. Parameters have been developed, which minimize the production of fines (less than 400 mesh) that tend to cause die sticking and lead to an increase in the general oxygen content of the powder.

Future Direction

- On an ongoing basis, perform the necessary process characterizations, such as dilatometry and chemical, thermo-gravimetric, microstructural, and x-ray diffraction (XRD) analyses required to develop sintering cycles for Ti-alloy powder compositions of potential interest to the automotive industry that yield high-density components.
- Complete static mechanical properties testing of pressed-and-sintered test compacts produced from the milled and lubricated powders discussed above.
- Identify one or more suitable "automotive" components on which to focus a demonstration fabrication study. Press and sinter the demonstration components in an industrial P/Mfacility to validate findings from the milling, die lubrication, and sintering investigations.
- Contract with ITP to produce a low-cost, metastable, beta-type alloy powder for potential automotive applications.
- Evaluate alternate low-cost Ti feedstocks for P/M or wrought (melt-processing) products.

Introduction

The use of low-cost ilmenite to produce the $TiCl_4$ employed in the ITP process was demonstrated in the previous reporting period. It was determined that the low-cost $TiCl_4$ did not adversely affect ITP's powder-synthesis process. However, during a series of high-rate die-pressing trials using commercial P/M equipment, it was determined that the low-purity powder would require further modification to mitigate the high friction forces measured in the pressing studies, eliminate die sticking through better control of powder size distribution, and establish robust sintering conditions that simultaneously accommodate current commercial practice. Thus, during this reporting period, three key studies were performed: 1) the sintering behaviors of the low- and high-purity powders, 2) an instrumented powder-pressing die was constructed and trials were performed to measure the forces that lead to high friction, and 3) a series of milling trials to determine how the powder size distribution could be properly modified.

Results and Discussion

Sintering Investigation

As part of this activity, a study was initiated last year to examine the use of low-cost, ilmenite-derived $TiCl_4$ as the precursor in Ti powder synthesis. The $TiCl_4$ was synthesized by DuPont at their TiO_2 pigment-production facility. However, unlike the high-purity chloride precursor used in pigment synthesis, the low-cost $TiCl_4$ underwent only one stage of distillation to remove iron chloride impurities. Both this source of $TiCl_4$, and a second, high-purity source (refined via the typical multistage distillation process) were employed in synthesizing CP-Ti using the Hunter process at DuPont and the Armstrong process at ITP.

As shown in Table 1, there is little difference in the concentrations of interstitial and key reduction-reaction by-product (i.e., NaCl) impurities between the high- and low-purity-Armstrong-produced powders. Similar results were observed in the Hunter materials. However, results from induction-coupled plasma/mass spectroscopy (ICP/MS) analysis did indicate that trace impurity elements transfer from the proprietary, single-stage, $TiCl_4$ distillation product to both forms of low-purity powder. Low- and high-magnification micrographs of the various powders, shown in Figure 1, indicate that little difference in particle morphology was observed between the high- and low-purity forms of each powder type. From Figure 1, it is apparent that both the Hunter and Armstrong powders are actually agglomerates composed of fine-scale crystallites. In general, the size of the constituent crystallites is smaller in the Hunter material than in the Armstrong-produced powders. The corresponding size distributions for the four different powder types are presented in Figure 2. Again, little difference was observed between the high- and low-purity versions of each powder type and the Hunter powder agglomerates tend to be several times smaller on average than the Armstrong powders.

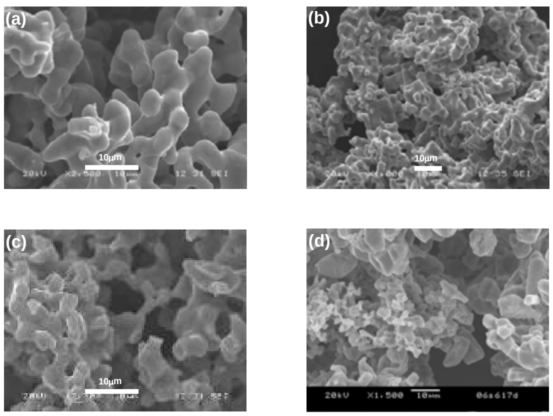

Figure 1. High-magnification images of: (a) high-purity Armstrong powder, (b) high-purity Hunter powder, (c) low-purity Armstrong powder, and (d) low-purity Hunter powder.

Element	High-purity Armstrong powder (ppm)	Low-purity Armstrong powder (ppm)
C	93	55
N	77	47
O	2400	1780
Na	330	110
Cl	19	21
BET (m^2/g)	0.31	0.31

Table 1. Concentration of interstitial and key reduction-reaction by-product (i.e., NaCl) impurities between the high- and low-purity, Armstrong-produced powders. BET = Specific surface area measurement.

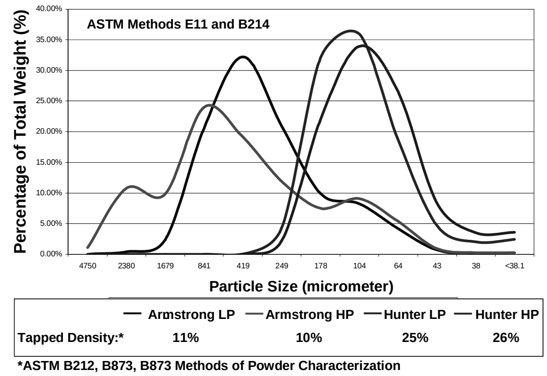

Figure 2. Particle-size distributions of high- and low-purity powders produced by the Armstrong and Hunter processes.

As discussed in the fiscal year (FY) 2006 annual report, prior dilatometry measurements indicated a significant difference in the sinterability of the high- and low-purity, Armstrong-produced materials. Specifically, in the high-purity powder, the onset of sintering takes place at ~400ºC whereas in the low-purity powder it is delayed to nearly 900ºC. Interestingly, however, tensile bars prepared from the high-purity powder exhibit substantially lower densities when sintered at 1250ºC than do comparable, low-purity specimens, as seen in the plot of as-sintered density vs. sintering time shown in Figure 3. A comparison of the internal microstructures of both specimen types in Figure 4 shows this difference more dramatically. As shown in Figure 5, swelling occurs in the high-purity specimens sintered for extended periods.

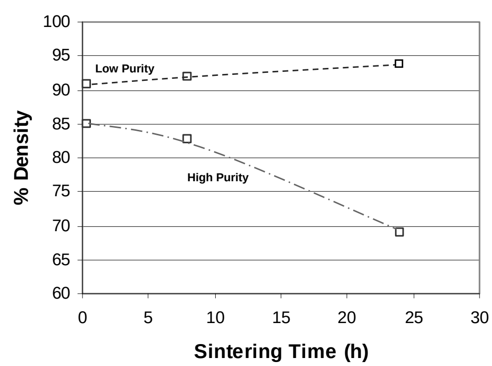

Figure 3. A plot of final density versus sintering time at 1250°C for two series of tensile specimens fabricated from high- and low-purity Armstrong powders.

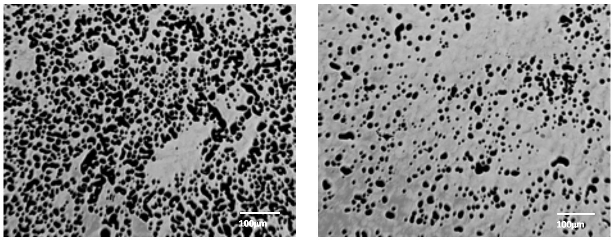

Figure 4. Cross-sectional scanning electron microscope (SEM) images of the internal microstructures of sintered bodies fabricated from: (a) high-purity and (b) low-purity Armstrong powders.

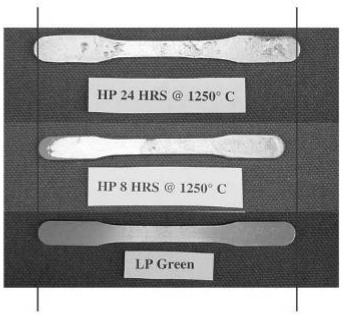

Figure 5. A comparison of the lengths of three tensile bars. Top two were prepared from high-purity Armstrong powder; bottom is representative of a tensile bar in the as-pressed condition.

At 1250ºC, the flow stress of CP-Ti is quite low (< 100 psi) i.e., the material will readily creep when placed under an external load or subjected to an internal pressure. It is suspected that a species susceptible to volatilization at high temperature (still undetermined) is present in the Armstrong-produced CP-Ti powder. If trapped within the Ti body during sintering, this species could lead to excessive pore formation and growth with the increase in time at elevated temperature. Recalling that the high-purity powder is far more sinterable than the low-purity material, it is, therefore, more prone to this type of entrapment/swelling mechanism, as shown schematically in Figure 6. Note that swelling has not been observed in Armstrong-produced Ti alloy powders (e.g., Ti-6Al4V) synthesized from high-purity $TiCl_4$, presumably because the alloying agents cause a delay in sintering that allows volatile species to escape the compact and avoid entrapment. The net effect is that the use of the lower-purity $TiCl_4$ source may be beneficial in two ways: (1) it is potentially a lower-cost precursor for use in Ti powder production and (2) the trace impurities allow higher-density components to be fabricated via a low-cost, press-and-sinter approach. Preliminary mechanical test results indicate that the impurities have no effect on tensile strength.

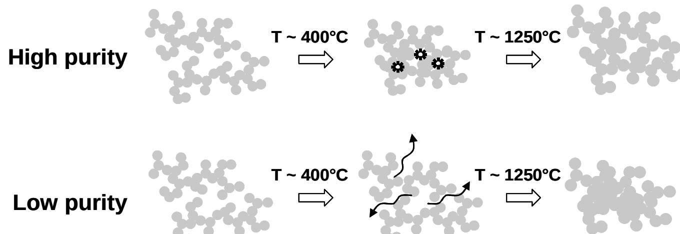

Figure 6. Schematic representations of the mechanisms speculated to occur during sintering of the high-purity and low-purity Armstrong processed CP-Ti powders.

Die Lubrication

In addition to the historically high material costs associated with Ti part manufacture, there are those inherent to conventional primary and secondary material processing, such as rolling, forging, and machining. One means of reducing production cost is to employ near-net-shape processing such as P/M techniques, where possible. A common P/M practice used in manufacturing small steel automotive parts (gears, pump bodies, etc.) is uniaxial die compaction. However, this has found limited application in fabricating high-quality Ti components because of the high powder and die-wall friction forces (i.e., particle/particle and particle/die-wall interactions) typically encountered during die compaction of Ti powder. High friction forces lead to inhomogeneous green densities, subsequent internal porosity, and part distortion during sintering. Porosity is particularly problematic in components designed for high fatigue life (i.e., springs and gears). In addition, excessive die-wall friction increases the force required to eject the part from the die cavity, which leads to increased die-wall galling, higher die wear, and shorter die life.

Both powder and die-wall friction can be reduced by incorporating an appropriate lubricant. The key is to identify a transient material that promotes the formation of high-density green bodies, yet is readily removed from the component prior to or during sintering, leaving behind no residual interstitial impurities (i.e., C, O, or N) that can embrittle the final part. Recognizing the potential economic value of effective P/M processing for Ti automotive components, an instrumented die was designed at PNNL to measure die-stress profiles *in-situ* during compaction and to evaluate the efficacy of various lubricants in increasing compact green density and reducing die wear. Shown schematically in Figure 7(a), is a cross-sectional view of the die. Thirteen, radially-aligned, strain-gage pinholes have been machined into the die along at 30° angular increments and 2.54-mm height intervals to form a helical radial-stress measurement array. As shown in Figure 7(b), the instrumented die employs a matching pair of punches and four linear springs to simulate the double-action compaction process commonly employed in industry. Continuous monitoring of top-punch position, compaction load, and radial die stress affords real-time analysis of both die-wall stress and die-wall and powder friction. As shown in Figure 7(c), radial stress is measured via strain-gage pins that are axially constrained between the die wall and a hollow setscrew at each of the thirteen hole locations.

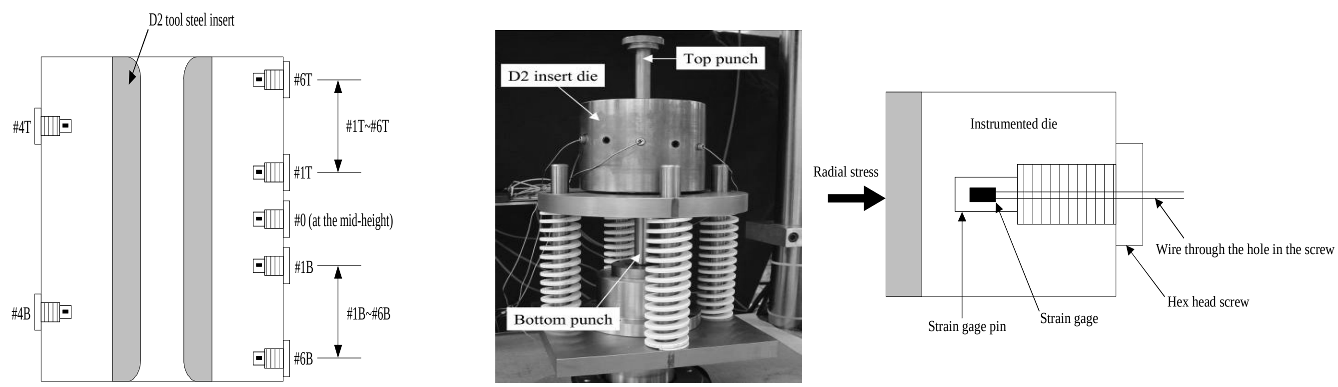

7(a) 7(b) 7(c)

Figure 7: (a) A schematic of the enhanced instrumented die: a cross-sectional side view. The strain-gage pin holes in the die are located helically with 30° angular and 2.54-mm height intervals. (b) The experimental set-up to simulate a double-action pressing. Two strain-gage pin holes were left open to clearly show the location of the holes. (c) A schematic of the assembly of a strain-gage pin and the enhanced instrumented die.

Using a pre-set maximum axial stress of 80 ksi, unmodified (i.e., no lubricant/binders added) Ti powder obtained from DuPont, Inc. CP-Ti powder produced as Hunter fines (apparent density = 0.87 g/cc, d_{50} ~ 131μm) was compacted to ~85% of theoretical density. For comparative analysis, a similar series of compactions was conducted using a commercial iron (Fe) powder obtained through Western Sintering, Inc. (blended with 0.75 wt% ethylene bistearamide wax, apparent density = 2.94 g/cc; d_{50} ~ 116μm), which compacted under the same axial stress to green densities averaging ~88% of theoretical. Shown in Figures 8(a) and (b) are the histories of the applied axial stress and the associated radial stress (measured at the vertical center of the die) as a function of time for the Ti and Fe powders, respectively. For both powders, the mid-height radial stress increases in nearly linear fashion with a linear increase in axial compaction stress. After a brief hold period, the axial stress drops to zero as the top punch is withdrawn for compact ejection. Note that a residual radial stress remains in each case due to friction between the powder particles within the compacts. In turn, this residual stress induces a die-wall frictional resistance force that must be overcome to eject the compacted part from the die. The radial stress generally decreases as the part is ejected. However, note that, for the Ti compact, there is a sharp increase in axial stress required for final ejection due to a higher static coefficient of friction for the Ti powder vis-à-vis Fe.

There is a correlation between the high ejection stress and the uniformity of radial stress in the green body both during the compaction and hold periods of the pressing process. Shown in Figure 9(a) are the radial stress profiles at maximum axial stress for the Ti and Fe powder compacts.

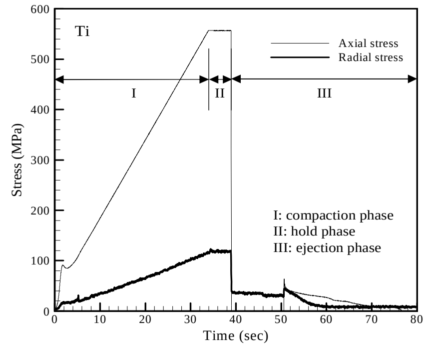

(a)

Figure 8. The histories of the applied axial stress and the radial stress, which was measured at the mid-height of the die, as functions of time for (a) the Ti powder and (b) the Fe powder.

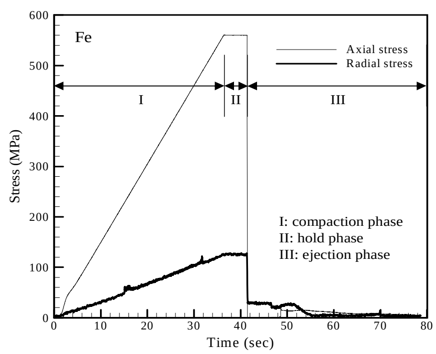

(b)

Note that for the Fe powder, the radial stress distribution is relatively uniform, which is not the case for the Ti material. The latter material displays a peak stress in the center of the compact, which is expected to be accompanied by a distinct gradient in density across the compact, i.e., also peaking at the center and tailing off near the top and bottom. Similarly, the graphs shown in Figure 9(b) display the residual radial-stress profiles for each compact recorded at the start of the hold period. Again, the profile measured from top to bottom for the Fe compact is uniform, while that for the Ti compact exhibits a maximum in the center of the body.

The Fe powder employed in these experiments is generally considered "ideal" for P/M processing via uniaxial die compaction. With that in mind, one of our objectives in lubricant selection for the

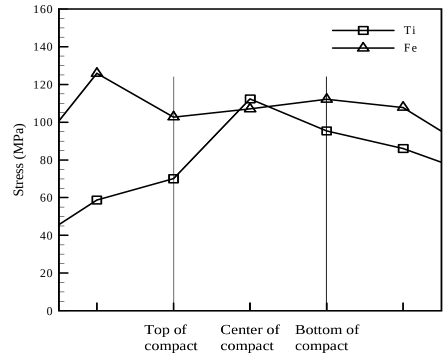

(a)

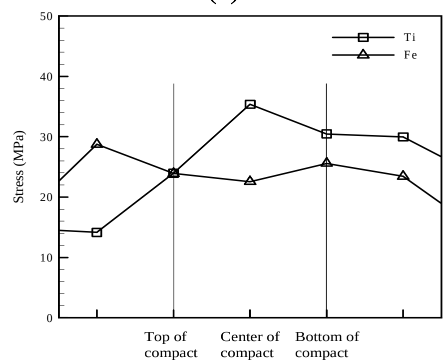

(b)

Figure 9. (a) Typical profiles of the radial stress at the limit axial stress for the CP-Ti and commercial Fe powders. (b) Typical profiles of the residual radial stress for the CP-Ti and commercial Fe powders. Note that each tick on the abscissas represents the stress measurement location of the die.

Ti powder is to duplicate the same type of pressing behavior in Ti as was observed with Fe, i.e., achieve moderately-low, residual, radial stresses and uniform radial stresses profiles during the compaction process and eliminate the spike in ejection stress. A series of polycyclic aromatic hydrocarbon (PAH) compounds was examined as potential powder lubricants, including: naphthalene, pyrene, anthracene, anthragallol, and camphor. In several cases, stearic acid (a well-known lubricant for Fe and copper (Cu) powders) was added as a secondary lubricant and a die-wall lubricant was employed. The PAHs were chosen because they are relatively easy to remove after powder compaction via sublimation under vacuum. To date, a series of 18 experiments has been conducted to explore the effects of powder lubricant composition and powder-to-lubricant ratio on radial stress distribution, die-wall friction distribution, and green density in CP-Ti compacts. While these experiments are still in the final stages of data acquisition, preliminary analysis indicates that both powder and die-wall lubrication can substantially improve the compaction behavior of Ti. For example, shown in Figures 10 and 11 are the compaction test results (at an applied axial pressure of 80 kpsi) for unmodified CP-Ti and CP-Ti mixed in a 10:1 ratio with camphor, both in comparison with the previously described commercial Fe powder. Note the greater uniformity in radial stress across the lubricated powder compact and the corresponding reduction in die-wall friction. This leads to an increase in green density of 3 – 5%, which, in turn, can increase the sintered density from ~90% of theoretical to 96 – 98% while extending the life of the die. Without optimization, the compaction behavior of the lubricated CP-Ti powder is similar to that of the commercial Fe powder. Future work will focus on measuring what effects these lubricants may have on material chemistry in the as-sintered state. It is anticipated that the use of PAH-based lubricants will not cause a measurable increase in the concentration of interstitial elements, in particular carbon.

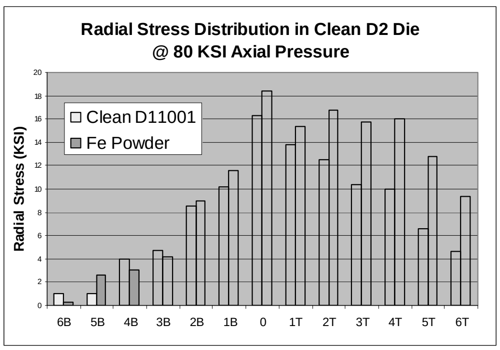

(a)

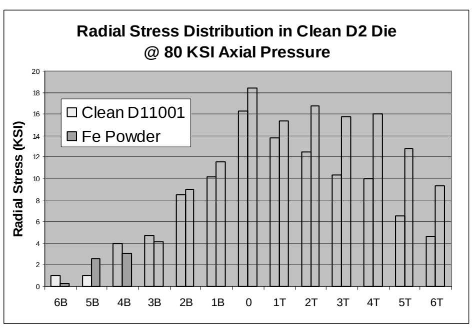

(b)

Figure 10. (a) Typical profiles of the radial stress at the limit axial stress for unmodified CP-Ti and commercial Fe powders. (b) Typical profiles of the die-wall friction for unmodified CP-Ti and commercial Fe powders.

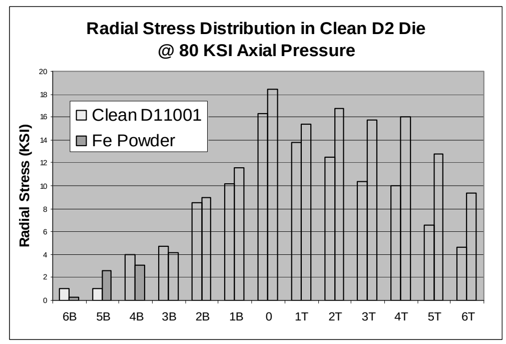

(a)

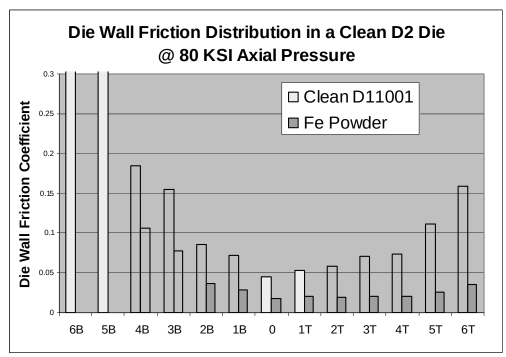

(b)

Figure 11. (a) Typical profiles of the radial stress at the limit axial stress for CP-Ti + camphor (10:1 volumetric ratio) and commercial Fe powders. (b) Typical profiles of the die-wall friction for CP-Ti + camphor (10:1 volumetric ratio) and commercial Fe powders.

Milling Studies

Although the ITP process has been demonstrated to produce high-quality Ti powder, the current size distribution will limit the potential automotive uses. The enhanced flow characteristics (as measured by the Hall meter in previous studies) and uniform die-fill required for very highly-detailed, net-shape automotive parts, will require additional milling of the powder. The challenge of milling the ITP Ti powder is to produce a size distribution that is fine enough to pour through the Hall meter without generating a large fraction of fine powders that increase interstitial element content and become trapped between the die and punch, causing die sticking (typically considered to be less than 400 mesh). Therefore, a study to modify, in a controlled manner, the particle size distribution was initiated. Milled powders were evaluated based on powder morphology, particle-size distribution and oxygen content. Three separate milling techniques were evaluated using variations of the applicable parameters of each methodology. High-energy Spex milling, low-energy ball milling, and high-production-throughput attrition milling were selected for the study. Each system was modified for milling operations to take place in an argon-rich environment.

Many parameters, including milling aids, time, media, and intensity, were evaluated and each milling process selected produced a powder size and morphology that poured easily through the Hall meter. The typical appearance of the powder produced by each method is shown optically in Figure 12. The most important finding was that ball-milling and attrition-milling compacted the agglomerates rather than fracturing the agglomerates, as was observed in the SPEX-milled powders. As expected, the attrition- and ball-milled powders produce fewer particles less than 230 mesh and had correspondingly lower oxygen content. Several iterations on the process parameters for the three milling methods have been made and, as reported previously, the high-intensity SPEX-milling process produced large fractions of fine powders and a nearly 2000 ppm increase in oxygen content and, as such, has been eliminated from the test matrix. A small sampling of the effectiveness of ball and attrition milling has been included in Figure 13, where samples of the powder, with equivalent particle distribution, are compared for oxygen content for powder sizes above and below 230 mesh. As shown by Figure 13, for powders of an equivalent powder size distribution, large differences in oxygen content were observed depending on parameters used. For example, attrition milling could produce powders that ranged in oxygen content from a minimum of 2500 to greater than 4200 ppm, for conditions labeled #3 and #1, respectively.

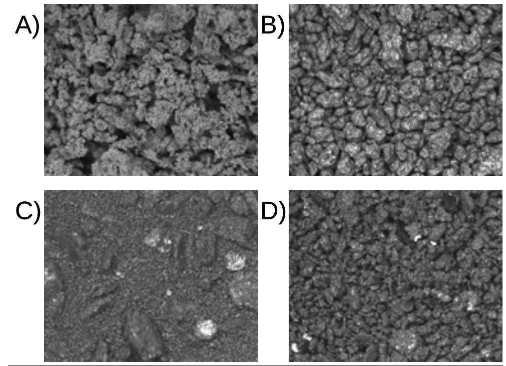

Figure 12. CP-Ti powder. A) As-received from ITP. B) Ball-milled powder. C) SPEX-milled powder. D) Attrition-milled powder.

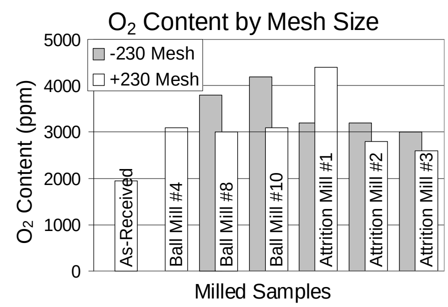

Figure 13. Chart comparing oxygen contents of Ti powders exposed to several milling conditions. The powders reported here were selected based on morphological similarity.

Conclusions

The low-purity powders produced by ITP are suitable for many bulk part applications and have been used in powder rolling and cold-hearth melting with a high degree of success. However, the highly-detailed parts used in automotive applications, such as valves, gears, springs, and fasteners that are candidates for Ti, require a finer, uniform powder distribution in order to meet the lowest part-cost, net-shape, P/M processing methods. During this reporting period, the following conclusions regarding the low-cost ITP powder for automotive P/M applications were reached:

- Sintering conditions that lead to increased part density can be established based on the proper control of the onset temperature for sintering.
- Die lubrication can be used to mitigate galling and, thereby, reduce part ejection forces,

potentially improve part quality, and reduce part cost by increasing die life.

- Similarly, admixed powder lubricants increase green body density and reduce part-ejection forces.
- Controlled powder-milling processes can yield particle-size distributions and oxygen contents that are suitable for high-volume P/M applications.

Publications/Patents

1. Lavender CA, and KS Weil. 2006. *Low-Cost Ti Powder for Feedstock.* Pacific Northwest National Laboratory, Richland, WA.
2. Lavender CA, 2007. *Cost-Effective Production of Powder Metallurgy Ti Components for High-Volume Commercial Applications.* Pacific Northwest National Laboratory, Richland, WA.
3. Lavender CA, 2007. *Low-Cost Ti Powder for Feedstock.* 2006 Annual Report: Automotive Lightweighting Materials. Pacific Northwest National Laboratory, Richland, WA.

Presentations

1. Hovanski Y, CA Lavender, KS Weil, and LA Jacobsen. 2007. *Net Shape Powder Metallurgy Processing Using ITP Ti Powder.* Presented by Yuri Hovanski at TMS 2007 Annual Meeting & Exhibition, Orlando, FL on February 27, 2007.
2. Weil K, Hovanski Y, and CA Lavender, 2007. *Investigation of Potentially Low-Cost Ti Powders for Use in Automotive Applications*. Presented by Scott Weil at TMS 2007 Annual Meeting & Exhibition, Orlando, FL on February 27, 2007.
3. *The Development of Low-Cost Ti Powder Processing,* Presented by CA Lavender at MS&T 2007 Detroit, September 10, 2007.
4. *Modification and Analysis of Ti Powders Synthesized by the Armstrong Process,* Presented by CA Lavender at MS&T 2007 Detroit, September 10, 2007.

B. Production of Heavy Vehicle Components from Low-Cost Titanium Powder

Co-Principal Investigator: Randall German
Director and Professor
Center for Advanced Vehicular Systems (CAVS)
Mississippi State University (MSST), P.O. Box 5405
Mississippi State, MS 39762-5405
(662) 325-5431; fax: (662) 325-5433; e-mail: german@cavs.msstate.edu

Co-Principal Investigator: Seong Jin Park
Associate Research Professor
CAVS, 2215
MSST, P.O. Box 5405
Mississippi State, MS 39762-5405
(662) 325-8565; fax: (662) 325-5433; e-mail: sjpark@cavs.msstate.edu

Co-Principal Investigator: Haitham El Kadiri
Assistant Research Professor
CAVS
MSST, P.O. Box 5405
Mississippi State, MS 39762-5405
(662) 325-5568; fax: (662) 325-5433; e-mail: elkadiri@cavs.msstate.edu

Co-Principal Investigator: Youssef Hammi
CAVS
MSST, P.O. Box 5405
Mississippi State, MS 39762-5405
(662) 325-5452; fax: (662) 325-5433; e-mail: yhammi@cavs.msstate.edu

Co-Principal Investigator: Paul T. Wang
Manager, Computational Manufacturing and Design
CAVS
MSST, P.O. Box 5405
Mississippi State, MS 39762-5405
(662) 325-2890; fax: (662) 325-5433; e-mail: pwang@cavs.msstate.edu

Co-Principal Investigator: Pavan Suri
Assistant Research Professor, CAVS
MSST
Mississippi State, MS 39762-5405
(662) 325-8278; fax: (662) 325-5433; e-mail: pks44@msstate.edu

Co-Principal Investigator: Craig A. Blue
Oak Ridge National Laboratory (ORNL)
Oak Ridge, TN 37831-8063
(865) 574-4351; fax: (865) 574-4357; e-mail: blueca@ornl.gov

Co-Principal Investigator: William H. Peter
ORNL
Oak Ridge, TN 37831-8063
(865) 241-8113; fax: (865) 574-4357; e-mail: peterwh@ornl.gov

Technology Area Development Manager: Joseph A. Carpenter
(202) 586-1022; fax: (202) 586-1600; e-mail: joseph.carpenter@ee.doe.gov

Expert Technical Monitor: Philip S. Sklad
(865) 574-5069; fax: (865) 574-6098; e-mail: skladps@ornl.gov

Contractor: MSST
Contract No.: 4000054701

Objective

Design and produce titanium (Ti) structural components by using math-based, experimentally-validated, powder-compaction and sinter models.

Approach

We examine lower-cost, blended-elemental (BE) and prealloyed (PA) Ti powders that are responsive to the powder metallurgy (P/M) process and synthesize new combinations and innovations in powder composition. Recent developments, such as using hydride powders, have enabled the fabrication of BE parts to over 99% of full density, resulting in significantly improved properties. Additives such as carbon or boron can then generate carbide or boride reinforcing phases – dispersed phase composites. Further studies and developments show that this approach may be well suited to reduce the cost of producing automotive parts, making Ti more cost-competitive with other materials commonly used. The work includes powder modifications, novel organo-metallic lubricants (the composition is proprietary), finite-element analysis of the compaction to minimize wall friction and wear, and evaluation of novel tooling materials and coatings. New computer tools for modeling porosity and size change during both compaction and sintering are tailored to Ti systems, with the ability of performing computer-aided design for the tooling and processes to attain dense and net-shaped final products.

Accomplishments

- Completed the literature survey for low-cost Ti powder, Ti alloys for automotive application with cost analysis, and their processing techniques.
- Designed new Ti alloys and proposed three Ti-alloy candidates.
- Continued development of simulation tools for powder injection molding (PIM), die compaction, sintering, hot isostatic pressing (HIPing), and incorporated optimization.

Future Direction

- Design and perform the experiments for PIM.
- Evaluate the proposed alloys in terms of processing windows and mechanical properties.
- Establish modeling and simulation with ORNL experiment data for die compaction, sintering, and HIPing.
- Select a cost-effective and better-preformed Ti alloy and fabricate a prototype component for demonstration.

Introduction

Lower-cost Ti could be the catalyst for Ti losing its perception as an expensive material and allow it to break into the automotive industry. The goal is to produce a market-competitive Ti component by low-cost manufacturing methods. The proposed research on Ti and Ti-matrix composites is the first step toward the application of P/M net-shape technology of lightweight materials into the domestic automotive industry. P/M techniques offer designers the flexibility of producing complex, near-net shape parts with the potential of significant cost savings due to very little waste in materials.

Table 1 shows the overall task structure, including the involvement of the ORNL team based on previous discussions between MSST and ORNL. Note that IAP Research will also provide hydride-dehydride (HDH) Ti powders with nanoscale additives for PIM.

Table 1. Overall structure of Task 1

	experiment	simulation
die compaction	ORNL	MSST
PIM	MSST	MSST
sintering	ORNL	MSST
HIPing	ORNL	MSST

Current Progress Based on Schedule Planned

Table 1 shows the current progress based on the schedule planned. Subtasks related to experiments are behind schedule now. We need experiment data from die compaction, sintering, and HIPing for modeling purposes. As for PIM, we need to find a sponge- powder supplier or obtain timely assistance from ORNL.

Table 2. The proposed schedule of Task 1 with marks of progresses

Subtasks	Year 1				Year 2			
	Q1	Q2	Q3	Q4	Q1	Q2	Q3	Q4
1.01 literature review, first simulation	100							
1.02 powder evaluation	100							
1.03 microstructure and interfacial study	80							
1.04 processing evaluation	80							
1.05 modeling and simulation		60						
1.06 optimization		30						
1.07 experimental verification		30						
1.08 mechanical properties and fatigue								
1.09 defect evaluation by non-destructive method								
1.10 corrosion and oxidation								
1.11 cost modeling								
1.12 process verification								

Summary of the Progress

The task consists of three research categories: literature survey, Ti-alloy design and evaluation, and modeling and simulation for Ti-powder processings.

Literature Survey

The literature survey was completed for Ti powder production methods of gas atomized, HDH, and sponge Ti powders, Ti alloys, P/M processes, and previous Ti alloys in use for automotive applications. The cost of Ti alloys is at least 10 times higher than the cost of aluminum (Al) alloys and 30 times higher than the cost of steels. Table 3 summarizes the consumption of Ti alloys in the automotive market between 1998 and 2002. It is seen that Ti alloys were never used in massive production mode. They were only limited to components requiring extra-high stiffness. For example, Ti is superior in maximum strength and fatigue strength scaled to density when compared to Al, magnesium (Mg), and steels. However, manufacturers show tendencies to use slightly-expensive Ti alloys rather than Al in the powertrain if rotating and oscillating masses in design are required to be substantially reduced.

Table 3. Ti alloys' uses in automotive applications

year	component	material	manufacturer
1998	brake guide pins	Grade 2	Mercedes
1998	sealing washers	Grade 1s	Volkswagen
1998	gear shift knob	Grade1	Honda
1999	connecting rods	Ti-6Al-4V	Porsche
1999	valves	Ti-6Al-4V	Toyota
1999	turbocharger rotor	Ti-6Al-4V	Mercedes
2000	suspension spring	LCB	Volkswagen
2000	valve cups	b-Ti alloy	Mitsubishi
2000	turbocharger rotor	g-TiAl	Mitsubishi
2001	exhaust system	Grade 2	GM
2002	valves	Ti-6Al-4V	Nissan

We also analyzed the cost for several Ti alloy candidates, as shown in Figure 1. This analysis indicates that the type of Ti powders (i.e., gas-atomized, HDH, and sponge Ti powders) is the most important factor in cost control.

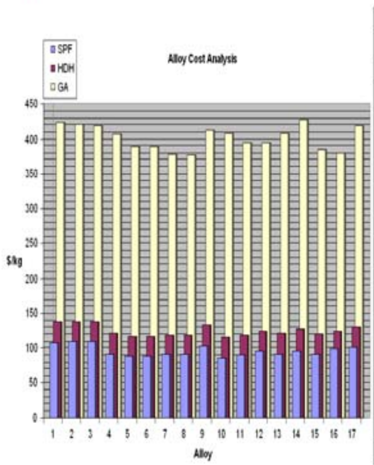

ID	Alloy Composition
1	Ti-6Al-4V
2	Ti-6Al-4V-1Mo
3	Ti-6Al-4V-1Mo-0.2B
4	Ti-8Al-1V-1Mo
5	Ti-6Al-2Sn-4Zr-2Mo
6	Ti-6Al-2Sn-4Zr-2Mo-0.2Si
7	Ti-6.5Al-4.6Sn-4.6Zr-1Nb-0.3Si-1Mo
8	Ti-6.6Al-4.6Sn-4.6Zr-0.9Nb-1Mo-0.35Si
9	Ti-4.5Al-3V-2Fe-2Mo
10	Ti-6Al-1.7Fe-0.1Si
11	Ti-4.5Fe-6.8Mo-1.5Al
12	Ti-1.5Fe-6.8Mo-4.8Al-1.2Nb
13	Ti-1Fe-1Mo-6.3Al-1.2Nb
14	Ti-1.5Fe-2.25Mo-1.2Nb-0.3Al
15	Ti-6Al-4Sn-4Zr-1Nb-1Mo-0.2Si
16	Ti-4.3Fe-7Mo-1.4Al-1.4V-5.4B
17	Ti-2Co-2Mo-1.4Al-1.4V-1.8B

Figure 1. Cost analysis plot for candidate Ti alloys.

Ti Alloys Design and Evaluation

Ti alloys can be a predominant monophase structure; α (hexagonal close-packed, hcp) or β (body-centered cubic, bcc), or a dual-phase structure α+β, depending on the composition strength ratio between the α stabilizing elements and β stabilizing elements. Figure 2 schematically illustrates the main properties of potential Ti alloys falling in different crystallographic classes. α alloys only enclose traces of β phase. Near-α alloys contained predominantly α and the microstructure may appear to be similar to an α alloy. A dual-phase, α-β alloy consists of α and retained or partially-transformed β. Metastable β alloys predominantly contain retained β, which is susceptible to a fine transformation upon post-heat treatments. All of these alloys are used for temperatures less than 600°C, although the melting temperature is higher than that of typical steel. The thermal expansion coefficient is less than half of Al.

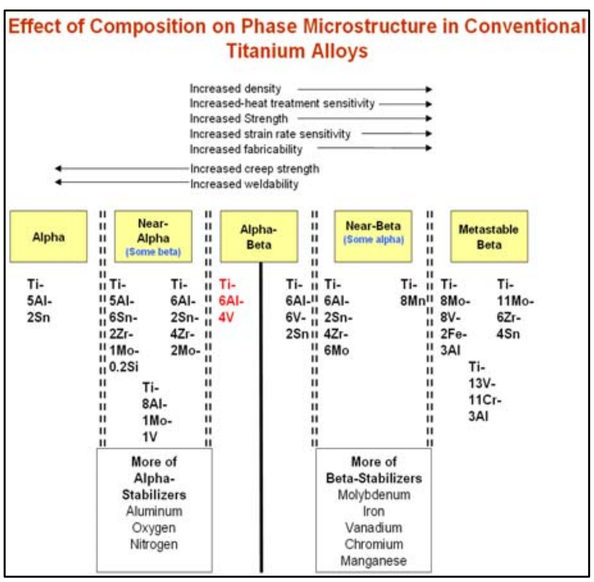

Figure 2. General classification of Ti alloys with respect to properties and microstructure.

Based on our research activity, we recommend starting with the following three compositions using a master-alloy powder for generating the eutectic systems:

I) Ti-(2 to 3%)Fe- (3% to 6%)Zr- (2% to 4%)Sn- (1% to 3%)Mo- (0% to 1%)Cr)

II) Ti-(2 to 3%)Fe- (3% to 6%)Zr- (2% to 4%)Sn- (2% to 3%)Mn- (1 to 2%)Mo- (0% to 1%)Cr)

III) Ti-(2 to 3%)Fe- (3% to 6%)Zr- (2% to 4%)Sn- (2% to 3%)Mn- (1 to 2%)Mo- (2% to 5%)Cr_3C_2.

Currently, we have purchased all required powders for evaluating the proposed Ti-alloy compositions. The evaluation will be performed through powder mixing, die compaction, sintering, and mechanical property measurement. Figure 3 shows the optimization algorithm for liquid-phase sintering of Ti-alloy powder.

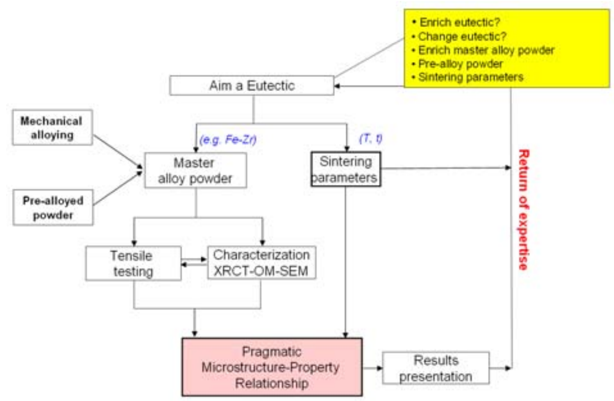

Figure 3. Composition optimization algorithm for liquid- phase sintering of Ti-alloy powder.

As for the PIM, we prepared PIM feedstock based on the standard, wax-polymer binder system with 50 % solid-loading percentage. We are now measuring the viscosity using a homemade capillary rheometer to obtain material properties for simulation.

Modeling and Simulation

PIM: We compared the flow behavior of three different Ti powders (gas atomized, HDH, and spherodized HDH Ti), as shown in Figure 4a. From the literature, material properties of HDH Ti powder for PIM were made available. We used PIMsolver® code donated by CetaTech, Inc. to simulate the PIM process. A tensile-specimen geometry was selected for simulation as shown in Figure 4b. The simulation results inferred possible processing windows (Figure 4c), and optimized the filling time for minimum injection pressure (Figure 4d).

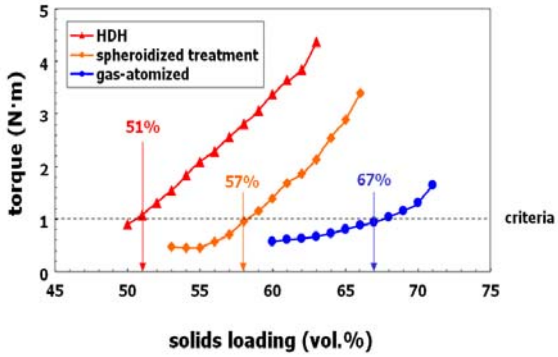

Figure 4a. Torque vs. solid loading.

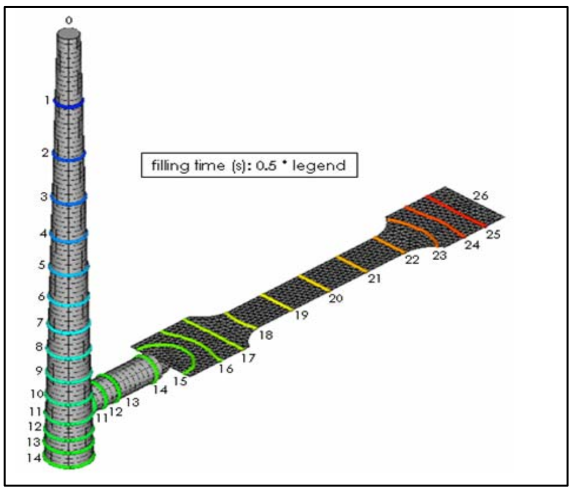

Figure 4b. Filling pattern.

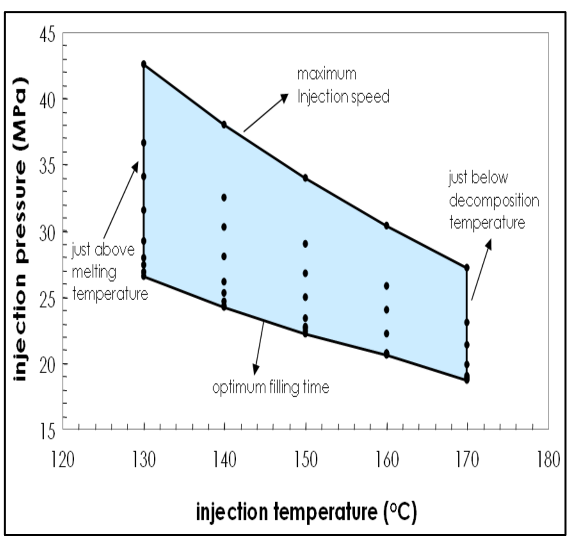

Figure 4c. Processing window

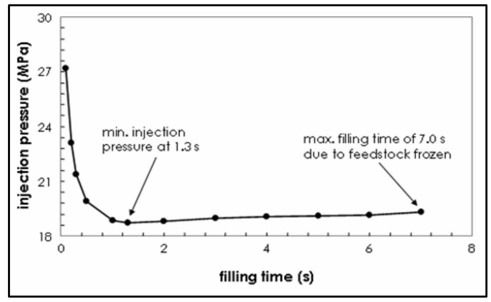

Figure 4d. Optimum filling time.

Figure 4. The first trial of PIM simulation and optimization with HDH Ti powder.

Die Compaction: We obtained all material properties of CP-Ti powder including the compressibility curve (Figure 5a) from literature for die-compaction simulation using ABAQUS. A gear geometry was considered as the first demonstration and simulations were performed, as shown in Figure 5b. In addition, we employed optimization algorithms to determine the loading schedule for reaching uniform green compact density.

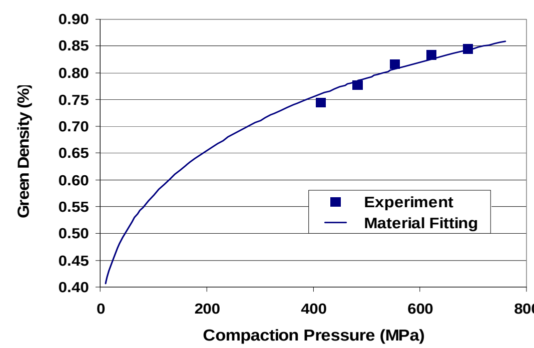

5a. Compressibility curve

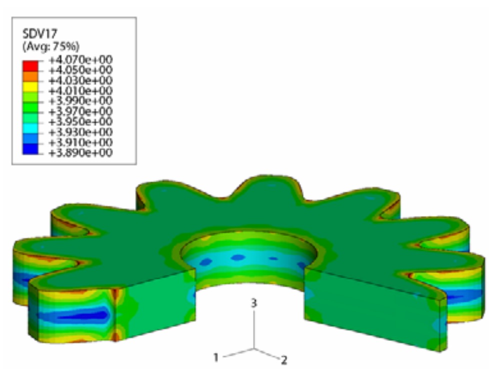

5b. Density distribution after compaction

Figure 5. The first trial of die-compaction simulation with CP-Ti powder.

Sintering and HIPing: We also have the capability to simulate sintering and HIPing processes. As for the HIPing, we obtained all material properties from a creep test with pressure and temperature dependency of Ti-6Al-4V powder and performed simulations of powder HIPing. In addition, we developed the algorithm to optimize can geometry to obtain accurate final HIPed component dimensions. Currently, we could not find through literature survey any Ti powder or Ti-alloy powder material properties for simulation of the sintering.

Conclusions

In the last six months, we accomplished the following (technically):

- Completed the literature survey for low-cost Ti powder, Ti alloys for automotive application with cost analysis, and their processing techniques.
- Designed new Ti alloys.
- Developed a simulation tool for powder injection molding, die compaction, sintering, and HIPing with some optimization.

Presentations/Publications/Patents

Conference Presentation:

1. Haitham El Kadiri, William Peter, Robert Whitehorn, Seong Jin Park, Youssef Hammi, Randall German, Craig Blue, Jim Kiggans, “Microstructure and Mechanical Properties of Sponge Ti and Its Alloy Powders with Various Powder Metallurgical Processes,” *TMS 2008*, March 9-13, 2008: New Orleans, LA.

Patents (in preparation)

Three Ti alloy compositions.

C. Powder-Metal Performance Modeling of Automotive Components (AMD 410[i])

Project Manager: Howard Sanderow
Management & Engineering Technologies (MET)
161 Copperfield Drive
Dayton, OH 45415
(937) 832-1583, fax: (937) 832-0858; e-mail: metgroup@earthlink.net

Principal Investigator: Mark F. Horstemeyer (Paul T. Wang, Youssef Hammi)
Center for Advanced Vehicle Systems (CAVS) Chair in Solid Mechanics & Professor, Mechanical Engineering
Mississippi State University (MSST)
206 Carpenter Bldg., P.O. Box ME
Mississippi State, MS 39762
(662) 325-7308; fax: (662) 325-7223; e-mail: mfhorst@me.msstate.edu

Russell Chernenkoff, (retired from Ford Motor Company)
Metaldyne Sintered Component, Inc.
Metaldyne Powertrain Global Operations and Technical Center
47603 Halyard Drive
Plymouth, MI 48170
(734) 582-6227, fax: (734) 582-6250; email: russellchernenkoff@metaldyne.com

Jean Lynn, Senior Specialist
Chrysler, LLC
800 Chrysler Drive, CIMS 482-00-15
Auburn Hills, MI 48326
(248) 512-4851; fax: (248) 576-7490; e-mail: jcl6@chrysler.com

Shekhar G. Wakade, Technical Specialist Materials Engineering
General Motors (GM)/ Powertrain
823 Joslyn Ave.
Pontiac, MI 48340
(313) 322-0175, fax: (248) 857-4425; e-mail: shekhar.g.wakade@gm.com

Glen Weber, Technical Specialist Engine Metals
Ford Motor Company
Building #1, Cube 12A037
Dearborn, MI
(248)) 568-1143; e-mail: gweber@ford.com

Technology Area Development Manager: Joseph A. Carpenter
(202) 586-1022; fax: (202) 586-1600; e-mail: joseph.carpenter@ee.doe.gov

Field Project Officer: Aaron D. Yocum
(304) 285-4852; fax: (304) 285-4403; e-mail: aaron.yocum@netl.doe.gov

Expert Technical Monitor: Philip S. Sklad
(865) 574-5069; fax: (865) 576-4963; e-mail: skladps@ornl.gov

Contractor: U.S. Automotive Materials Partnership (USAMP)[i]
Contract No.: DE-FC26-02OR22910 through the National Energy Technology Laboratory

Objective

- The objective is to develop and experimentally validate math-based models for powder-metallurgy (P/M) component design and performance prediction. The effort will extend an existing USAMP microstructure-property model from casting to PM for practical application in low strain-rate (design and durability) and high strain-rate (toughness-driven impact strength) environments. This model will be used to evaluate and optimize an automotive-component design (main-bearing cap) as affected by materials (ferrous and non-ferrous) and manufacturing processes (compaction and sintering). This model will be implemented into various software platforms (such as ABAQUS). It will be robust enough to facilitate the insertion of various lightweight materials such as aluminum (Al) and titanium (Ti) for future component applications.

Approach

- Determine current PM standards publications, component-design guidelines, manufacturing, and evaluation methodologies. Provide a selection of metal powders that can satisfy design-performance requirements, component-design guidelines, and manufacturing and testing specifications across industry participants (Task 1).
- Evaluate and develop numerical-modeling techniques to predict mechanical properties throughout P/M-component sections. The transition of current materials/design requirements to advanced, structural P/M components has created a need to predict the properties of components in all sections of design. In addition, design processes should consider the least-cost, lowest-mass product designs and reduced development lead-time. An existing, math-based framework will be extended with the abilities to predict P/M-component structures and properties accurately throughout the compaction and sintering processes (section size, density variation, dimensional tolerances, potential for cracking) and with the input of alloys and process parameters (machine functions, tool and powder temperatures, friction and pressure). It will capture the history of a P/M part through its pressing, sintering, and life-cycle performance using the developed multiscale methodology (Task 2).
- Develop component- and vehicle-level testing to validate durability, quality control and performance of P/M parts. Quality-control process factors (powder properties, press settings, tooling design, and furnace conditions) will be determined for P/M parts production in terms of their impacts on process variations and quality improvement. Optimization and statistical techniques will be used to help determine the main factors affecting the final component. Validation experiments considering actual boundary conditions from real processes to fracture the components will be performed (Task 3).
- Manage and report program activities: There will be bi-weekly teleconferences and two technical review sessions per year. Intermittent meetings will be held throughout the year to report progress and discuss issues. Proper execution of this task will greatly enhance the visibility and the value of this project. Reports generated from this program will follow the guidelines suggested by Department of Energy (DOE) and United States Council for Automotive Research (USCAR) (Task 4).
- Perform technology/commercial-transfer throughout the product value-chain. To date, there exists limited accountability for major research and development (R&D)/technical institutions to foster the infrastructure to support large-scale applications of P/M components. If the auto industry wishes to take advantage of P/M's potential weight and cost-reduction opportunities, they must nurture P/M development through programs sponsored and directed by USCAR. The project team will request the professional support of societies to publish notices of meetings and project information, as released by the project team (Task 5).

Accomplishments

- Continued to characterize powder and green-compact, comprising FC-0205 Ancorsteel powder provided by Hoeganaes and 205Q powders provided by Metaldyne. Obtained structure/property data during sintering on FC-0205 and 205Q powders (Task 2).
- Measured the density distributions of the green and sintered main-bearing caps provided by Metaldyne using immersion density and image analysis. Measured the density distribution of the sintered main-bearing cap using the two-dimensional (2D) x-ray computed tomography (CT) (Task 3).
- Compaction Modeling Status: Validated modeling and simulation efforts for cylindrical samples under compaction with Al 6061, tungsten carbide and FC-0205 experimental data. Validation on Cincinnati part and on main-bearing cap are ongoing (Task 2).
- Sintering Modeling Status: Developed and implemented in ABAQUS/Standard code (Task 2).
- Received from Metaldyne 205Q and 223 powders, transverse rupture strength (TRS) test bars and bearing caps in green and sintered conditions. Also received tensile bars and material samples to be machined into tension, compression, torsion and fatigue specimens (Task 3).
- Performed tension, compression, torsion, notched and smooth fatigue tests on samples provided by Metaldyne to calibrate the internal state variable (ISV) performance model and a fatigue model (Task 3).
- Hosted meetings at CAVS with USCAR P/M team members in March, August and December 2007 (Tasks 4-5).
- Submitted two conference papers at PowderMet2007 (Task 4).
- Completed semi-annual and annual reports for release to USCAR and DOE (Task 4).

Work Plan for 2008

- Enhance the compaction model with additional features, i.e., springback responses during ejection (March 2008).
- Correlate the FC-0205 and 205Q sintering data with the models (February 2008).
- Validate the experimental results on the main-bearing cap with the sintering simulation results (February 2008).
- Validate the plasticity/fatigue model with the information provided by Metaldyne – main-bearing cap. (April 2008).
- Use the model to optimize the compaction and sintering processes for a main-bearing cap (April 2008)
- Apply the modeling to lightweight material such Al powder using literature data and predict the performance and fatigue property in a bearing cap (May 2008).
- Tech Transfer and Training (April 2008).

Introduction

The objective of this project is to develop and experimentally validate math-based models for P/M component design and performance prediction.

During this past year, different powder material tests have been conducted on the FC-0205 and 205Q powders to characterize and calibrate the compaction, sintering and performance parameters. The characterizations of the FC-0205 and 205Q powders during compaction and sintering are nearly completed. Using the 205Q powder material samples from Metaldyne (powder, TRS bars, tensile bars, material blanks and bearing caps), CAVS has performed tensile, compression, torsion and fatigue tests at different densities. Three different methods of density measurements have been used to determine the density distribution of the green and sintered bearing caps.

Regarding the modeling, the compaction model has been validated on cylindrical, Cincinnati and main-bearing cap (MBC) parts. Data from the literature and other material were used to validate the model as well. The compaction model for the ejection stage is currently being implemented. The sintering model has been developed, implemented and tested for algorithm efficiency.

Powder Characterization

A number of experimental tests and density measurements have been performed to gather the data necessary for characterization and validation of the constitutive equations of compaction and sintering. A brief description of these experimental tests follows.

Brazilian and Compression Tests

To determine material cohesion and interparticle-friction parameters, d and β, compression and Brazilian disc tests were performed on cylindrical green samples of different densities ranging from 5.2 to 7.3 g/cc [Coube and Riedel, 2000]. Two different FC-0205 powders were tested: powder 1 and powder 2 with 0.6% and 1.0% Acrawax, respectively. The Brazilian tests were performed according to American Society for Testing and Materials (ASTM) D3967-95a (2005): Standard Test Method for Splitting Tensile Strength of Intact Rock Core Specimens. The compression tests were performed according to ASTM E9-89a: Standard Test Methods of Compression Testing of Metallic Materials at Room Temperature. The fracture stresses, σ_c and σ_t, were measured in these two tests with different degrees of stress multiaxiality (Figure 1).

Closed-die Compaction Tests

The goal of this experiment is to determine the cap eccentricity parameter in the Cap Model. Six strain gages were attached to the external surface of a 2-inch-diameter steel die to measure the hoop strain. Gages 3 and 4 were located at the same distance from the bottom of the die. Compaction tests were performed on several FC-0205 powder cylinders of 0.5-inch diameter with different heights. The cap-eccentricity parameter in the Cap Model was determined with an inverse method by comparing the numerical hoop to measure the hoop strain. Gages 3 and 4 were located at the same distance from the bottom of the die. Compaction tests were performed on several FC-0205 powder cylinders of 0.5-inch diameter with different heights. The cap- eccentricity parameter in the Cap Model was determined with an inverse method by comparing the numerical hoop strains to the measured hoop strains at different locations on the die as illustrated in Figure 2.

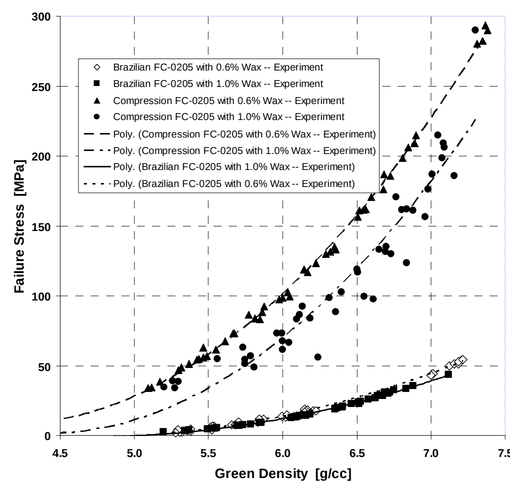

Figure 1. Failure stress vs. green density for FC-0205 cylindrical samples.

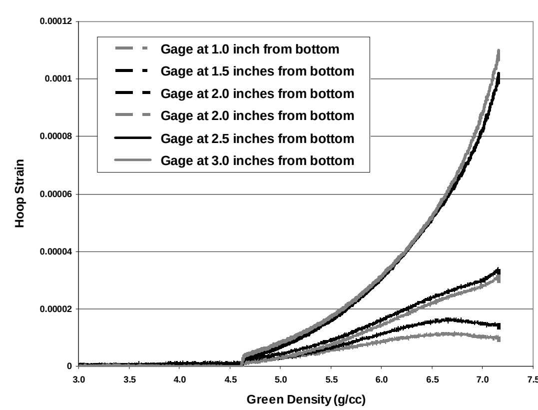

Figure 2. Experimentally-measured hoop strains for FC-0205 cylindrical samples.

The equivalent stresses, q_c and q_t, and the hydrostatic stresses, p_c and p_t, are calculated from the interpolation of the fracture stresses to determine the ordinate (*d*) and slope (tan β) of the straight-line failure envelope in the Drucker–Prager Cap Model at different densities (Figures 3 and 4).

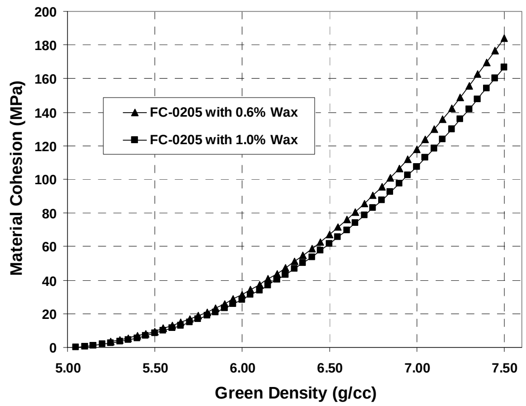

Figure 3. Material cohesion (*d*) vs. green density for FC-0205 cylindrical samples.

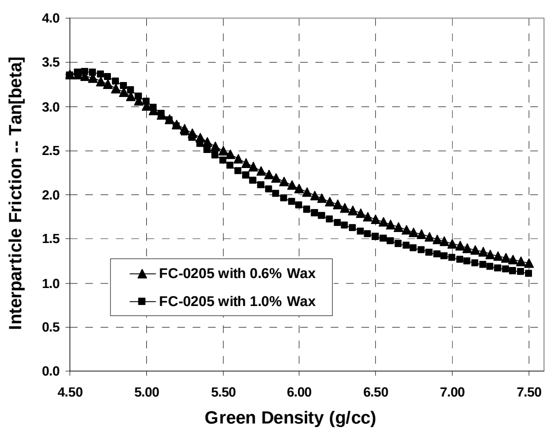

Figure 4. Interparticle friction (tan β) vs. green density for FC-0205 cylindrical samples.

Resonant Frequency Tests

Using the resonant frequency method [Yu et al., 1992, McIntire, 1991], the Ultra RS laboratory in France determined the Young's modulus, *E,* and Poisson ratio, ν, of FC-0205 rectangular bars sized 1.25 in x 0.5 in x 0.25 in. with green densities ranging from 5.6 to 7.2 g/cc [Figure 5]. The bulk modulus, *K*, and shear modulus, *G*, were then derived from the *E* and ν functions of density.

Density Measurements

Green-density measurements were made on the first press trial of the Cincinnati, Inc. samples. The first three sample parts of this press trial were cut into quarters. Each quarter was then further divided into twelve pieces (Figure 6), resulting in forty-eight total pieces for each sample part.

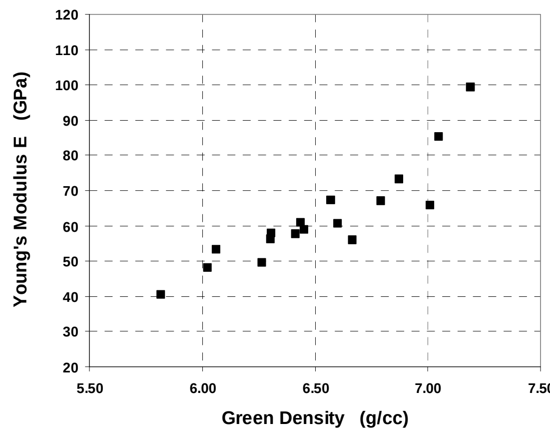

Figure 5. Young's modulus, E, as function of the density for the FC-0205 powder.

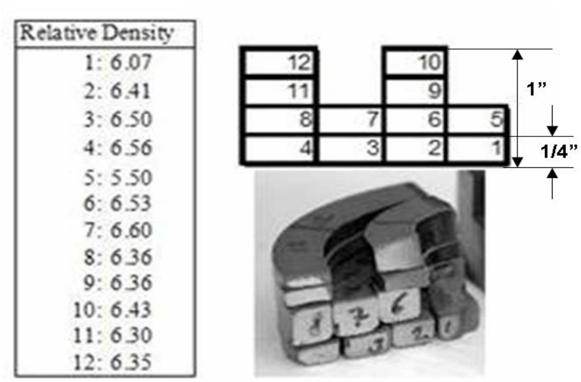

Figure 6. Average green-density map for the first press trial of the Cincinnati, Inc. sample part.

The green density for each piece was determined using the immersion density method (also called Archimedes' method) according to Metal Powder Industries Federation (MPIF) Standard 42: Method for Determination of Density of Compacted or Sintered Powder Metallurgy Products. By averaging the density measurements for the three parts, the green-density map for the

Cincinnati Inc. sample part of the first press trial was constructed (Figure 6).

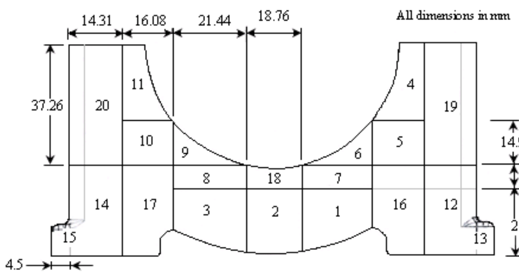

Figure 7a. MBC dimensions and location of the 20 samples.

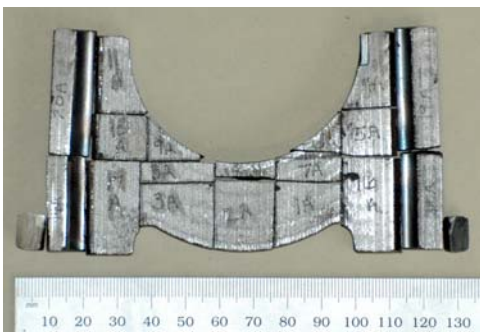

Figure 7b. Layer A of green MBC cut into 20 samples.

For the Metaldyne MBC, three different methods, image analysis, Archimedes' immersion and 2D X-Ray CT, were used to measure the green and sintered density. The same layering and sectioning of the MBC part was applied to all methods. Regarding the image analysis, a test procedure was developed specifically for the MBC. The MBC was sectioned into three layers of equal thickness. Each layer was further cut into 20 pieces, shown in Figures 7a and 7b.

In the image analysis procedure, the samples were mounted and then polished. Several images were captured for each of the 20 samples, using a Zeiss Axiovert 200MAT optical microscope with a motorized stage. A MATLAB program developed at CAVS was used as an image post-processor to overlay the porosity in red and output the total pore area of each image. The density of each sample was quantified using the void-area fraction, which is the ratio of void area to the representative sample area. In the 2D X-Ray CT technique, the X-ray image shows variations in photographic density between different parts of the object being scanned. In order to obtain density data, the gray-scale values of a CT image are correlated to known density values of different TRS samples using exactly the same scanning conditions. The gray-scale values in the CT are then converted to density values using a MATLAB image-processing program. This technique has the advantage of being a quick method to evaluate the relative density variations in the large P/M parts.

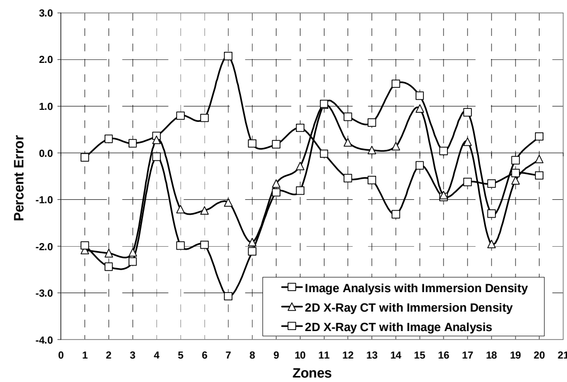

Figure 8. Percent error between the different density measurement methods for the layer A of the green MBC part.

Figure 8 shows the percent error between the three techniques. It is observed that the density measurement results from the immersion density and image analysis are very close. The percent error is given by

$$\%\ Error = \frac{D_1 - D_2}{D_2} \cdot 100 \qquad (1)$$

where D_1 and D_2 are the values of the two compared methods (the second density D_2 is assumed to be the "correct" value).

Dilatometry Test

The dilatometry test is a technique to measure the dimensional changes of a porous body continuously during sintering by using a probe or pushrod to measure the shrinkage or expansion of the sample *in situ*. Changes in the rate of shrinkage are linked to microstructural evolution and thermophysical events or chemical reactions [Blaine et al., 2005]. Dilatometry tests were performed on FC-0205 delubed compacts with a N_2 atmosphere. The compacts were heated at different constant heating rates (2°C/min, 5°C/min and 10°C/min) to 1120°C (2048°F) with a holding time of 30 minutes. The cooling rate was 10^{o}C/min. The observed variation in sintering shrinkage will be used to calibrate sintering parameters and to verify the predictive capability of the model (Figure 9). It is worthwhile to mention that the real sintering conditions are twice as fast as those shown in Figure 9.

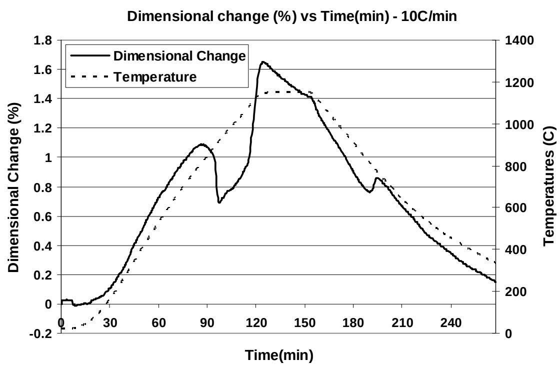

Figure 9. Dilatometer plots of axial shrinkage versus time for FC-0205 presintered compacts heated at a rate of 10°C/min to 1200°C in N_2 atmosphere.

To investigate the material grain-growth behavior, several sintering experiments on FC-0205 and 205Q powders were performed using three different heating rates and holding temperatures. The goal is to obtain the grain-growth rates graphically from the grain size against holding time plots for calibrating the grain-growth parameters.

Modeling

Compaction

The compaction model that was implemented in ABAQUS/Explicit was initially validated using literature data on Al-6061 Al powder. The FC-0205 parameters were calibrated using the p-q plot, which defines the evolution of the yield surface based on experimental data from Brazilian and compression tests, isostatic tests, and closed-die compaction tests.

The compaction was first validated using the FC-0205 parameters on cylindrical specimens by comparing the final average density from numerical results and experimental measurements. The model was then validated on more complex parts, such as the Cincinnati and MBC parts using, respectively, axisymmetric and hexahedral elements to represent the powder (Figure 10 and 11). To avoid numerical instabilities during the compaction simulation, two different numerical techniques were used. The Arbitrary Eulerian Lagrangian (ALE) adaptive meshing was applied to elements in order to control the mesh distortion. The no-separation relationship, which prevents the contact surfaces in interaction from separating once they have come into contact, was also applied to remove an unrealistic gap between the powder and the tool surfaces.

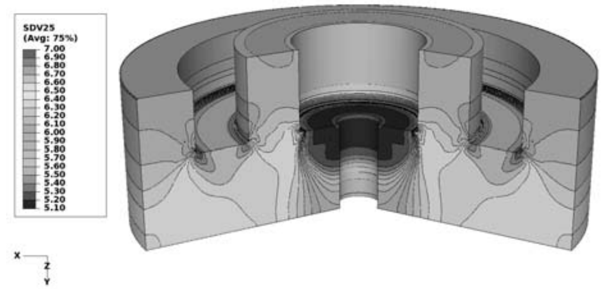

Figure 10. Density distribution (g/cc) in the Cincinnati part (axisymmetric model with swept display).

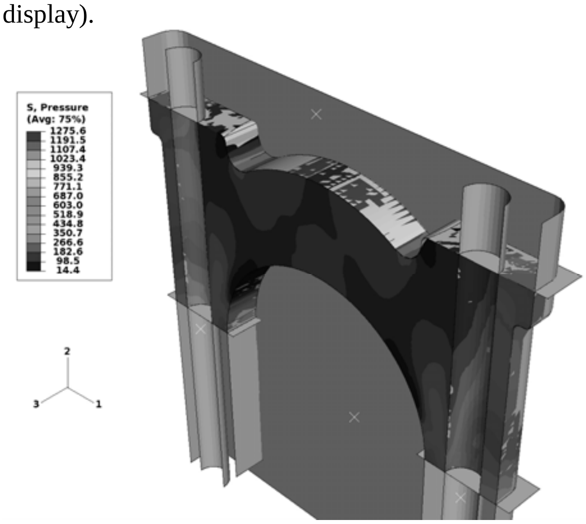

Figure 11. Pressure distribution (MPa) in the MBC part.

To validate the density distribution of the Cincinnati simulations, the density was averaged on several axisymmetric or hexahedral elements in volumes that correspond to the cut pieces for the immersion density method. Figure 12 shows the percent error of the average density from finite-element analysis (FEA) results compared with the immersion density values for the Cincinnati part. For the MBC simulation, CAVS is currently working with Metaldyne to determine the initial conditions and tool motions in order to improve the simulation results (Figure 13).

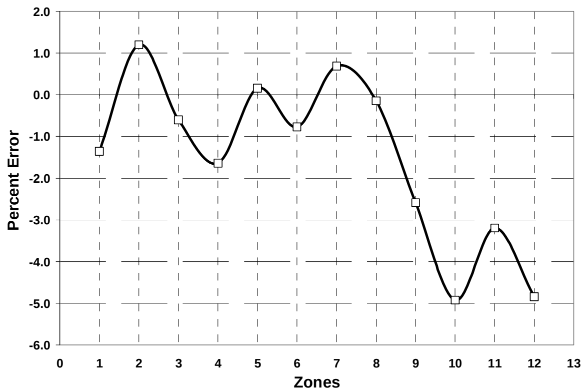

Figure 12. Percent error of the density values from finite-element analysis compared with density immersion measurement for the 12 pieces of the Cincinnati part.

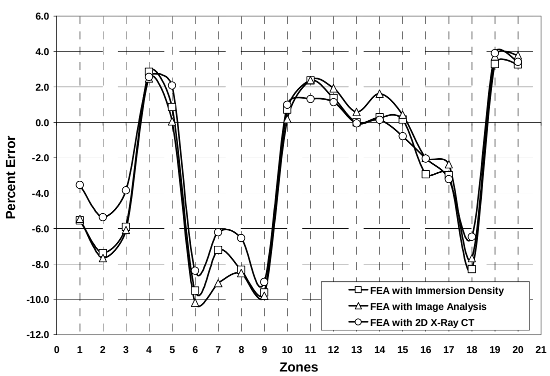

Figure 13. Percent error of the density values from FEA compared with different density measurement for the 20 pieces of the MBC part.

Sintering

To study the creep of powder due to diffusional mass transport on the interparticle contacts, a sintering model was implemented in the user-material subroutine UMAT of ABAQUS/Standard. This model is described by a macroscopic creep law that was initially proposed McMeeking and Kuhn [1992]. In the thermodynamic framework, to obtain the diffusional deformation rate as defined by McMeeking and Kuhn [1992], the following sintering dissipation potential was introduced:

$$F_{di} = -\frac{p}{K_d}\left(\frac{p}{2} + \sigma_s\right) + \frac{q^2}{6\mu_d}, \qquad (2)$$

where p and q are the first and second stress invariants, K_d and μ_d are shear and bulk viscosity, respectively, and σ_s is the sintering stress which arises from the surface tension forces of the pores. The densification rate is given by:

$$\underline{D}^{di} = -\frac{1}{3}\frac{p + \sigma_s}{K_d}\underline{I} + \frac{q}{3\mu_d}\underline{n}. \qquad (3)$$

where $\underline{I}$ and $\underline{n}$ are the unit tensor and plastic normal tensor. The stress-like term σ_s is the macroscopic manifestation of the driving forces for the processes of sintering. It is also called the sintering potential and is defined for different phases of the material [Kwon et al., 2004].

The viscosities μ_d and K_d are averages over the microstructure of the deformation processes within the particles and on interparticle boundaries [German, 1996].

The grain-growth evolution under pressureless sintering can be written as [Kwon et al., 2004]

$$\dot{G} = k'/G^2 \qquad (4)$$

where G is the grain size and k' is a material constant which can be determined from experimental data as a function of temperature.

The stress integration algorithm proposed by Govindarajan and Aravas [1994] was used to solve the sintering constitutive equations and compute the tangent consistent matrix.

The model was successfully tested using 17-4 PH stainless-steel parameters to evaluate the convergence efficiency and the robustness of the stress-integration algorithm. The next step will be to calibrate the FC-0205 and 205Q parameters using the dilatometry and void-growth data for complete validation of the sintering model.

Partnership with Metaldyne

Following the agreement between Metaldyne Sintered Component, Inc. and the Center for Powder Metal Technology (CPMT)/CAVS, Metaldyne provided to CAVS the following items:

- Geometry of a GM MBC: part drawing, tool geometry in IGES format, and fill, mold and ejection position drawings.
- 205Q and 223 powder bucket of 50 lbs.
- 205Q and 223 green and sintered TRS bars of different densities
- 205Q tensile bars of densities ranging from 6.4 to 7.2 g/cc.
- 205Q material blanks of different thickness and densities to be machined into material samples for tension, compression, torsion and fatigue testing.
- 50 green and sintered MBC parts made from 223 powder.
- 100 green and 90 sintered MBC parts made from 205Q powder.

Performance Testing

Model-calibration testing has been performed on monotonic and fatigue specimens machined from 205Q material blanks provided by Metaldyne. Monotonic experiments were conducted to capture stress-state dependence, temperature dependence, and strain-rate dependence. The various stress states were compression, tension, and torsion. Temperature dependence was accomplished by performing the tests at both 293K and 593K, and strain rates at 0.0001/s and 2000/s for strain-rate dependency. To date, compression tests have been performed at both temperatures and strain rates. Tension has been tested at 0.0001/s and both temperatures. Torsion testing has been performed at 293K and 0.0001/s.

The test data obtained have been used to develop one set of constants for a microstructure-based ISV. A plot of low-density and high-density specimen experiments tested to date along with the model curves are shown in Figures 14 and 15, respectively.

Fatigue calibration experiments were performed on round specimens with the same two density levels as used in the monotonic experiments. Loading was applied under strain control with completely reversed strain amplitude.
Specimens were cyclically tested by first applying a strain in tension, then uniaxially reloading in compression. The strain amplitudes tested for the high-density specimens were: 0.4%, 0.3%, 0.2%, 0.175%, 0.15%, and 0.1%. The low-density strain levels were 0.3%, 0.2%, 0.15%, 0.125%, and 0.1%. A frequency of 2 Hz was used when testing at strain amplitudes of 0.15% and higher. For the lower strain amplitudes, 0.125% and 0.1%, a frequency of 3 Hz was utilized.

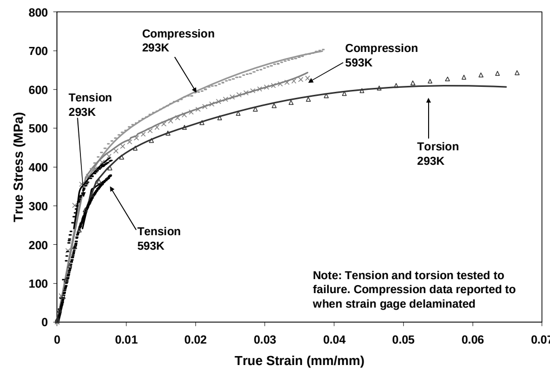

Figure 14. Low-density stress-strain showing the model (solid lines) plotted with the experimental data curves (dash lines).

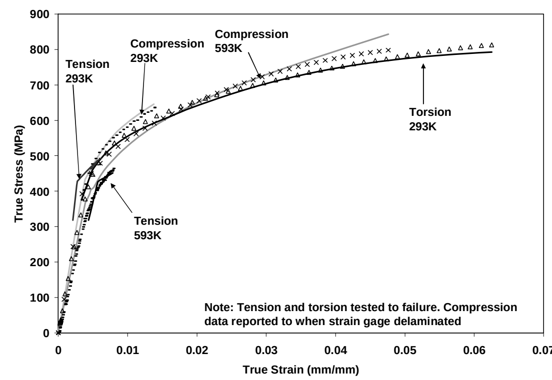

Figure 15. High-density stress-strain showing the model (solid lines) plotted with the experimental data curves (dash lines).

The fatigue experimental data were loaded into a microstructural-based ISV, multi-stage fatigue model. Figure 16 shows a strain-life plot of the experimental-data and model curve.

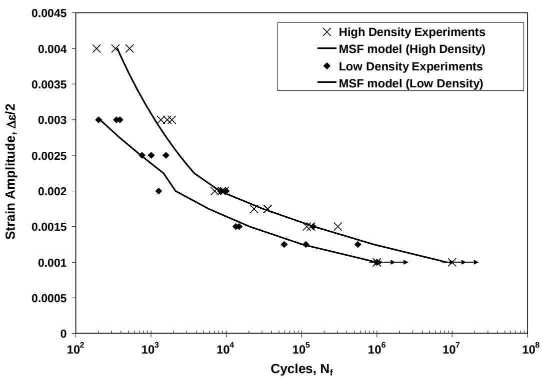

Figure 16. Strain-life fatigue experimental and multistage fatigue model comparison.

Conclusions

Determination of the microstructure-property relations and parameter calibration for the Powder-Metal Performance Modeling of Automotive Components project are almost completed except for the sintering-parameter calibration, which requires a more complicated procedure. The compaction model was validated with cylindrical and Cincinnati parts and partly with MBC parts; the numerical densities were in good agreement with the measured densities. The internal-state sintering and performance models have been developed and implemented. The ejection feature for the compaction model is being implemented and near completion. Therefore, having completed most of the material characterization and numerical developments, CAVS soon will be able to perform simulations of compaction and sintering for design, performance and mass optimization of the MBC. The final task will be the evaluation of lightweight materials in the MBC parts.

Publications

1. Allison P.G., Hammi Y. and Horstemeyer M.F., Determination of Microstructure-Property Relations for Performance and Design Optimization of the P/M Process", PowderMet 2007 conference, Denver, CO, May 13-16 2007, Vol. 1, Part 1.
2. Stone T.W., Jelinek B., Gullett P.M., Kim S.G., and Horstemeyer M.F., "MD Simulations of the Compressive Behavior of α-Fe and Fe-Cu Nanocrystalline Materials", PowderMet 2007 conference, Denver, CO, May 13-16 2007, Vol. 1, Part 1.

Acknowledgements

The authors would like to acknowledge funding from the Center for Advanced Vehicular Systems at Mississippi State University and from USAMP Advanced Materials Division (AMD). We thank Michael O'Neill, Ernie Bertolasio and Edmund Ilia from Metaldyne Sintered Components for all the information and material samples they provided us.

References

1. ABAQUS, User's Manual, Version 5.8, Hibbit, Karson & Sorensen, Inc., 2003.
2. Blaine, D., German, R., and Park, S., "Computer Modeling of Distortion and Densification during Liquid Phase Sintering of High-Performance Materials", Proceedings of the 2005 International Conference on Powder Metallurgy and Particulate Materials, Metal Powder Industries Federation, Princeton, NJ, 2005, 1.29-1.37.
3. Coube, O. and Riedel, H. "Numerical Simulation of Metal Powder Die Compaction with Special Consideration of Cracking", Powder Metallurgy, Vol. 43, No. 2, 2000, pp. 123–131.
4. German, R.M., Sintering Theory and Practice, Wiley and Sons, 1996.
5. Govindarajan, R.M., and Aravas, N., "Deformation processing of metal powders: Part II – Hot isostatic pressing", Int. J. Mech Sci. Vol. 36, No. 4, 1994, pp. 359-372.
6. Kwon, Y.S., Wu, Y., Suri, P. and German, R.M., "Simulation of the Sintering Densification and Shrinkage Behavior of Powder Injection Molded 17-4PH Stainless Steel," Metal. Mater. Trans., 2004, pp. 257–263.
7. McMeeking, R.M., and Kuhn, L.T., "A Diffusional Creep Law for Powder Compacts," Acta Metal. Mat., Vol. 40, 1992, pp. 961–969.
8. McIntire, P. (ed.), Nondestructive Testing Handbook, Volume 7, American Society for Nondestructive Testing, 1991, pp. 398-402.

9. Yu, C.J., Henry, R.J., Prucher, T., Parthasarathi, S., Jo J., 1992. "Reasonant frequency measurements for the determination of elastic properties of P/M components", Proceedings of the P/M'92 World Congress, Vol. 6, pp. 319–332.

---

[i] Denotes project 410 of the Automotive Materials Division (AMD) of the United States Automotive Materials Partnership (USAMP, www.uscar.org), one of the formal consortia of the United States Council for Automotive Research (USCAR) set up by Chrysler, Ford and General Motors (GM) to conduct joint, pre-competitive research and development.

D. Examining Fundamental Mechanisms of Tooling Wear for Powder Processing

Co-Principal Investigator: Seong Jin Park
Associate Research Professor
Center for Advanced Vehicular Systems (CAVS), 2215
Mississippi State University (MSST), P.O. Box 5405
Mississippi State, MS 39762-5405
(662) 325-8565; fax: (662) 324-4001; e-mail: sjpark@cavs.msstate.edu

Co-Principal Investigator: Randall German
Director and Professor
CAVS
MSST, P.O. Box 5405
Mississippi State, MS 39762-5405
(662) 325-5431; fax: (662) 323-3906; e-mail: german@cavs.msstate.edu

Co-Principal Investigator: Youssef Hammi
CAVS
MSST, P.O. Box 5405
Mississippi State, MS 39762-5405
(662) 325-5452; e-mail: yhammi@cavs.msstate.edu

Co-Principal Investigator: Paul T. Wang
Manager, Computational Manufacturing and Design
CAVS
MSST, P.O. Box 5405
Mississippi State, MS 39762-5405
(662) 325-2890; fax: (662) 325-5433; e-mail: pwang@cavs.msstate.edu

Technology Area Development Manager: Joseph A. Carpenter
(202) 586-1022; fax: (202) 586-1600; e-mail: joseph.carpenter@ee.doe.gov

Contract Monitor: Aaron Yocum
(304) 285-4852; fax: (304) 285-4403; e-mail: aaron.yocum@netl.doe.gov

---

Contractor: Mississippi State University (MSST)
Contract No.: 4000054701

Objective

- Develop an innovative design of tooling surfaces and novel lubricants for processing ferrous and lightweight materials.

Approach

- Productivity and performance of powder metallurgy (P/M) parts rely on the behavior of surface oxide which, by nature, is a dispersion-strengthened product. This work plans to use coated powders to provide an opportunity to control tool friction, surface reactions, and component strength. This research will apply new tools to the old problem of aluminum (Al) P/M. It relies on powder changes, alloying, and processing optimization to produce nearly full-density products with complex shapes and dimensional precision. The work is fundamentally new, since very little efforts have been focused on moving forward the lightweight automotive components fabricated by P/M for meeting desirable property levels as comparable with traditional ferrous P/M. Significant progress is expected in the key areas such as the optimal particle size distribution, powder coatings, active lubricants, and computer simulations.

Accomplishments

- Developed a new methodology to quantify tool wear for die compaction in the mold using silicon rubber.
- Proposed a new integral equation to quantify tool wear from numerical simulation results.
- Characterized the effect of lubricant on tool wear.
- Obtained industry sponsor in-kind support including CetaTech, AMPAL, Gasbarre products, Arburg, and CM Furnaces.
- Published one journal paper and five conference papers related to this task.
- Produced one master degree through this task.

Future Direction

- Work with Oak Ridge National Laboratory (ORNL) wear test facility use through the High-Temperature Materials Laboratory (HTML)/ORNL user program.
- Developed full design and optimization algorithm.
- Evaluate mechanical performance including fatigue and high strain-rate experiment.

Introduction

P/M techniques are widely used to fabricate complex automotive components from ferrous powders. The energy efficiency and cost attributes of P/M are recognized by the domestic automotive industry. Al P/M emerged in the 1950s, but current tonnage in the USA is trivial. With the push for lighter-weight, higher-strength, more-durable structures, the barriers to Al P/M in domestic automobiles need to be addressed. Besides economics, the technical barriers are: tool wear, performance, and ductility at high strain rates (related to crashworthiness).

In this sense, the goal of this project is to examine fundamental mechanisms of wear in die compaction with priority and to synthesize new combinations or innovations in powders, lubricants, press operation, and compaction cycles to minimize tool wear with integration of experimentation and numerical simulation.

Current Progress Based on Schedule Planned

All subtasks are progressed well, as shown in the Table 1 below.

Table 1. The proposed project schedule with marks of progresses

Sub Task	Year 1				Year 2			
	Q1	Q2	Q3	Q4	Q1	Q2	Q3	Q4
5.1	100%							
5.2	100%							
5.3	100%							
5.4	90%							
5.5		100%						
5.6			100%					
5.7			40%					
5.8				30%				
5.9								

Summary of the Progress

This project comprises three research categories: die wear measurement, Al-alloy evaluation, and modeling and simulation for tool wear.

Die Wear Measurement

We proposed, established, and are developing a new methodology to quantify tool wear during die compaction (Figure 1a) through a nondestructive method using RepliSet (Figure 1b) and a TalySurf profilometer (Figure 1c).

Once the methodology was set up, we calibrated silicon-rubber technique and found that its resolution was ±0.5 µm. Now we are measuring tool wear with three die-tool materials and four different powders including die diameter, die weight, surface roughness, and so on for quantifying tool wear. In addition, the microstructure was evaluated using scanning electron microscopy (SEM) as shown in Figure 2.

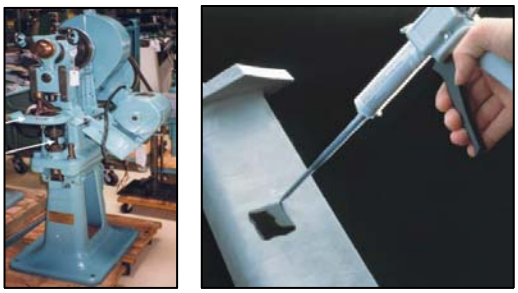

(a) (b)

(c)

Figure 1. Establishment of new methodology to quantify tool wear; (a) compaction machine with die for wear measurement, (b) RepliSet (silicon rubber and shot gun), and (c) TalySurf profilometer for surface measurement.

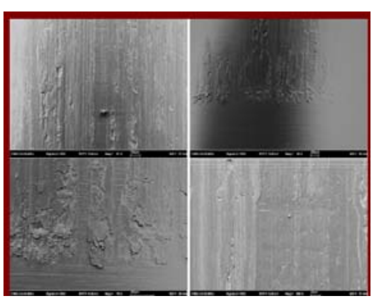

Figure 2. SEM image of silicon rubber surface to investigate ability of transcription of RepliSet.

Al-Alloys Evaluation

To obtain an Al alloy with excellent mechanical properties, we are evaluating nine different Al alloys with Mg, Cu, Si, SiC, and Ti. Especially, Al 6061 powder produced by rapid solidification, ATMIX, Japan, seemed to have a great potential so far. Our observation includes differential scanning calorimetry / thermogravimetric analysis (DSC/TGA) of mixed powder for phase transformation and melting; die- compaction and sintering behaviors through compressibility-curve and dilatometry tests; mechanical property measurements such as density, hardness with comparison (Figure 3a), and transverse rupture strength (TRS); and microstructure-evolution analysis using SEM pictures (Figure 3b). Furthermore, we just did the first trial of high-rate Hopkinson bar testing which is related to potential structural component analysis for crashworthiness.

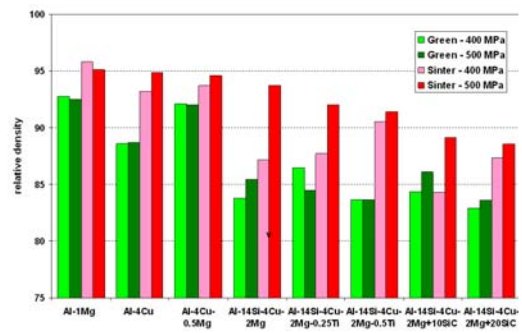

(a) Comparison of mechanical properties

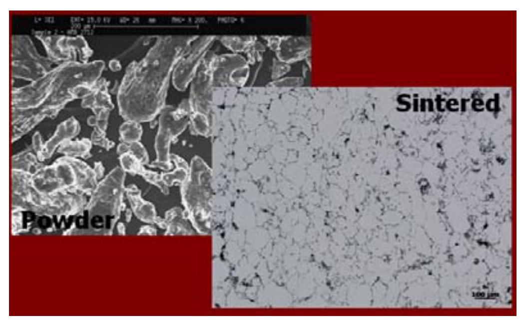

(b) SEM image of powder and sintered compact

Figure 3. Results of Al alloys evaluation.

Modeling and Simulation for Tool Wear

In order to take advantage of our simulation capability, we have proposed a new concept of wear work in integral form based on finite-element modeling (FEM) simulation results of die compaction and ejection as follows:

$$M = H(k_1 S_1 + k_2 S_2)W$$

and

$$W = \int_t \mu \int_A \sigma_n dA v dt$$

where M is the amount of tool wear, H is the Vickers harness number of tool material, k is the proportional constant, S is surface area of compact contacted with die tool, subscript 1 is for Al powder and 2 is for hard additives such as alumina (Al_2O_3) or silicon carbide (SiC), W is the wear work, μ is the friction coefficient, σ_n is the normal stress to die tool surface, A is the surface area, v is the velocity of the powder compact, and t is the time. We applied this definition to developed FEM simulation tool for die compaction and ejection with experiment validation to investigate the effect of die compaction and ejection stage with different friction coefficient as shown in Figures 4 and 5.

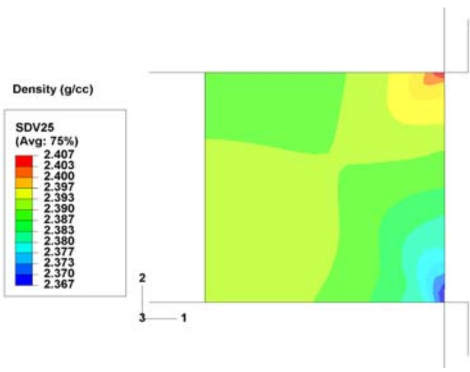

(a) density distribution

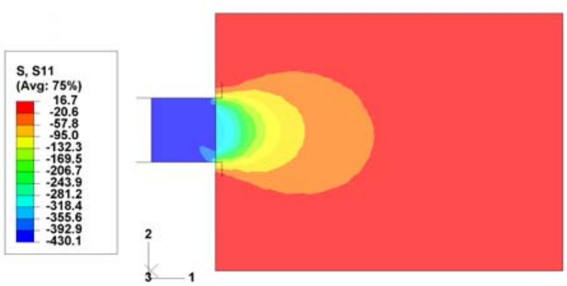

(b) stress distribution with die tool deformation

Figure 4. FEM simulation result.

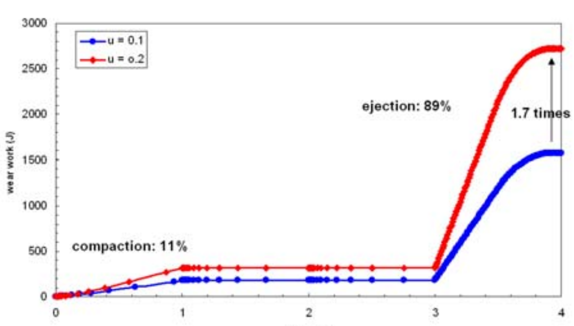

Figure 5. The effect of die compaction and ejection stage with different friction coefficient on tool wear.

We also investigated the effect of lubricant using FEM simulation. We used acrawax as the first trial with different amount of addition compared with results without lubricant, as shown in Figure 6, in term of compressibility and its effect on amount of tool wear.

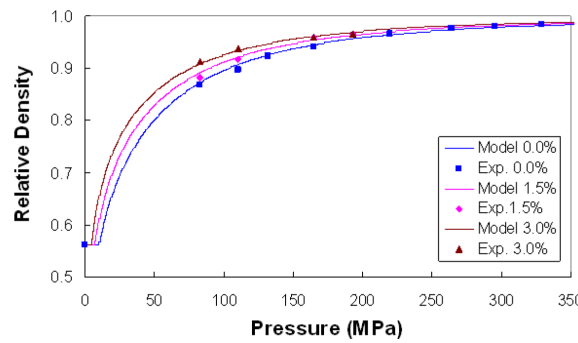

Figure 6. The effect of the amount of lubricant on compressibility of die compaction.

Conclusions

Last year, we produced one MS degree (James K. Thompson) through this project. In addition, we have accomplished the following technically:

- Developed a new, nondestructive methodology to quantify tool wear for die compaction in the mold using silicon rubber.
- Proposed a new integral equation to quantify tool wear from numerical simulation results.
- Characterized the effect of lubricant on tool wear.
- Published one journal paper and five conference papers related to this project.

Presentations/Publications/Patents

Journal Papers:

1. Suk Hwan Chung, Young-Sam Kwon, Seong Jin Park, and Randall M. German, "Sensitivity Analysis by the Adjoint Variable Method for Optimization of the Die Compaction Process in Particulate Materials Processing," Submitted for publication to ASME J. Eng. Mater. Tech., 2007.

Conference Presentations:

1. Arockiasamy Antonyraj, Seong Park, and Randall German, "Mechanical Properties of Various Aluminum Alloys by Powder Metallurgy," to be presented in TMS 2008, March 9-13, 2008: New Orleans, LA.
2. Seong Jin Park, Seong-Gon Kim, Mark Horstemeyer, and Randall M. German, "Multiscale Modeling in Powder Metallurgy: Atomistic, Discrete Element, and Finite Element Simulations," UKC (US – Korea Conference) 2007, August 9-12, 2007, Washington DC.
3. A. Antonyraj, Seong Jin Park, and Randall M .German, "Thermal Expansion and Viscoelastic Properties of Sintered Porous Ferrous Components," Proceedings of the 2007 International Conference on Powder Metallurgy & Particulate Materials (PowderMet 2007), complied by John Engquist and Thomas F. Murphy, Metal Powder Industries Federation and APMI International, Princeton, NJ, USA, Part 1, pp. 60-69, Denver, CO, USA, May 13-16, 2007.
4. James. K. Thompson, Seong Jin Park, Randall M. German, Fehim Findik, and Arockiasamy Antonyraj, "Novel Methodology to Quantify Tool Wear in Powder Metallurgy," Proceedings of the 2007 International Conference on Powder Metallurgy & Particulate Materials (PowderMet 2007), complied by John Engquist and Thomas F. Murphy, Metal Powder Industries Federation and APMI International, Princeton, NJ, USA, Part 1, pp. 50-59, Denver, CO, USA, May 13-16, 2007.
5. Fehim Findik, James K. Thompson, Arockiasamy Antonyraj, Seong Jin Park, and Randall M. German, "Mechanical and Physical Properties of Titanium and Silicon Carbide Containing Mixed Powder Sintered Aluminum," Proceedings of the 2007 International Conference on Powder Metallurgy & Particulate Materials (PowderMet 2007), complied by John Engquist and Thomas F. Murphy, Metal Powder Industries Federation and APMI International, Princeton, NJ, USA, Part 10, pp. 103-113, Denver, CO, USA, May 13-16, 2007.